INTERIM REPORT

Accession No. _____

Contract Program or Project Title: Light Water Reactor Thermal Hydraulic Development Program

Subject of this Document: Informal Report, "BNL Instrumentation Program"

Type of Document: Informal Report

Author(s): N. Abuaf, G. A. Zimmer, and O. C. Jones, Jr.

Date of Document: April 1979

Responsible NRC Individual and NRC Office or Division: Dr. Y. Y. Hsu
Division of Reactor Safety Research
Systems Engineering Branch
U. S. Nuclear Regulatory Commission
Washington, D. C. 20555

This document was prepared primarily for preliminary or internal use. It has not received full review and approval. Since there may be substantive changes, this document should not be considered final.

Brookhaven National Laboratory
Upton, NY 11973
Associated Universities, Inc.
for the
U.S. Department of Energy

Prepared for
U.S. Nuclear Regulatory Commission
Washington, D. C. 20555
Under Interagency Agreement EY-76-C-02-0016
NRC FIN No. A- 3045

BNL-NUREG -26051
INFORMAL REPORT

BNL INSTRUMENTATION RESEARCH PROGRAM

By

N. Abuaf, G. A. Zimmer, and O. C. Jones, Jr.

Reactor Safety Experimental Modeling Group

Date Published - April 1979

DEPARTMENT OF NUCLEAR ENERGY BROOKHAVEN NATIONAL LABORATORY
UPTON, NEW YORK 11973

Prepared for the U.S. Nuclear Regulatory Commission
Office of Nuclear Regulatory Research
Contract No. EY-76-C-02-0016

NOTICE

BNL-NUREG-26051
INFORMAL REPORT
LIMITED DISTRIBUTION

BNL INSTRUMENTATION RESEARCH PROGRAM

By

N. Abuaf, G. A. Zimmer, O. C. Jones, Jr.

Reactor Safety Programs
Thermal Hydraulic Development Division
Department of Nuclear Energy
Brookhaven National Laboratory
Upton, New York 11973

APRIL 1979

Prepared for the U.S. Nuclear Regulatory Commission
Office of Nuclear Reactor Regulation
Contract No. EY-76-C-02-0016
FIN NO. A-3045

TABLE OF CONTENTS

INTRODUCTION

The objective of the BNL Light Water Reactor Development Program is to obtain measurements of the volumetric vapor generation rates in flashing steam-water flows under steady and transient conditions of interest in accident analysis. Instrumentation in support of this activity was developed and constructed to obtain both local and global measurements of the appropriate information, i.e., void fraction and phase velocities. The methods described include local instruments (optical and r-f probes) that provide local information and a global densitometer using γ attenuation techniques. A minicomputer based data acquisition and data analysis system was also developed including a block signal analysis system with the proper time and frequency domain data manipulation software. This presentation summarizes the current status of the work and the accomplishments.

LOCAL PROBES

Local instruments for measuring the local void fractions and interphase passage velocities, consist of the optical probe and the r-f probe.

a. The optical probe. Three optical probe configurations have been used in the literature (Miller and Mitchie, 1969; Danel and Delhaye, 1971; Hinata, 1972). Three problems were identified common to all the probes mentioned above and were encountered in interpreting the local probe output: i) the electronic response of the system for fast moving small bubbles, ii) the hydrodynamic response of the probe tip, resulting in different penetration times of the probe into the bubble and back into the liquid. These penetration times were also observed to vary with the bubble size and

interface velocities, iii) the bubble dynamics,where following the streamlines, bubbles may at low velocities escape the probe tip and are not registered.

Based on preliminary considerations (Jones, 1977; Abuaf and Swoboda, 1977a), the construction techniques of an optical probe with a different tip geometry was developed and is documented in Figure 1 (Abuaf and Swoboda, 1977b). Figure 2 represents the schematic of the probe, the light source, and the photodiode, amplifier circuit (rise time of 20 μsec). The electronic response of the system was checked by means of a light emitting diode (LED) placed in front of the probe tip. The LED output was modulated by using a signal generator so that light pulses of different widths were emitted at various frequencies to simulate the passage of bubbles. The hydrodynamic response of the probe was investigated in an experimental set-up presented in Figure 3. It consists of a glass tube (0.64 cm I.D. and 83 cm long) through which different size bubbles can be accelerated to various velocities (8 cm/s - 280 cm/s) by means of a pressurized water column. Typical oscillograms of the probe output are depicted in Figure 4, showing the response to water, air and passage of the bubble. The ratio of the probe signal amplitude at various bubble velocities to the signal amplitude in air, under steady conditions is seen to decrease with the bubble velocity (Figure 5), for two probes having the same tip geometry.

Concerning the bubble penetration times, at high bubble velocities, the data follow a 1/v variation, but for low velocities (< 50 cm/sec) they become longer than the 1/v predictions, showing a possible surface tension dominance (Figure 6).

402 271

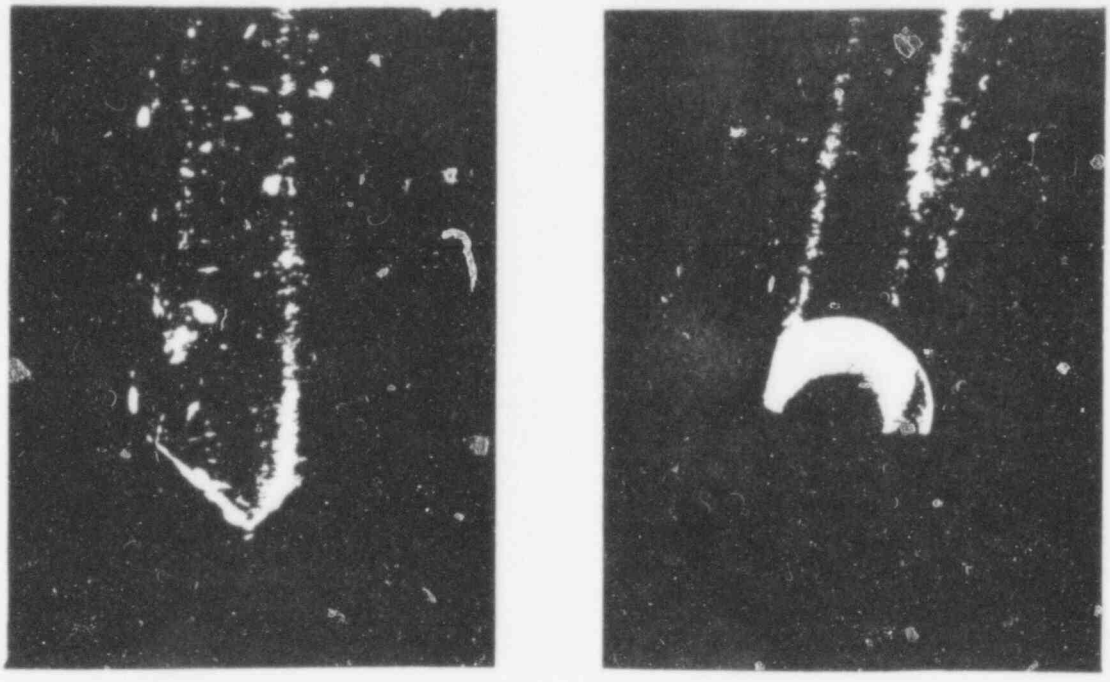

Figure 1. Straight edge optical probe tip geometry.
Stainless steel tube O.D. = 0.5 mm.
Optical fiber diameter = 0.125 mm.
(BNL Neg. No 4-911-78)

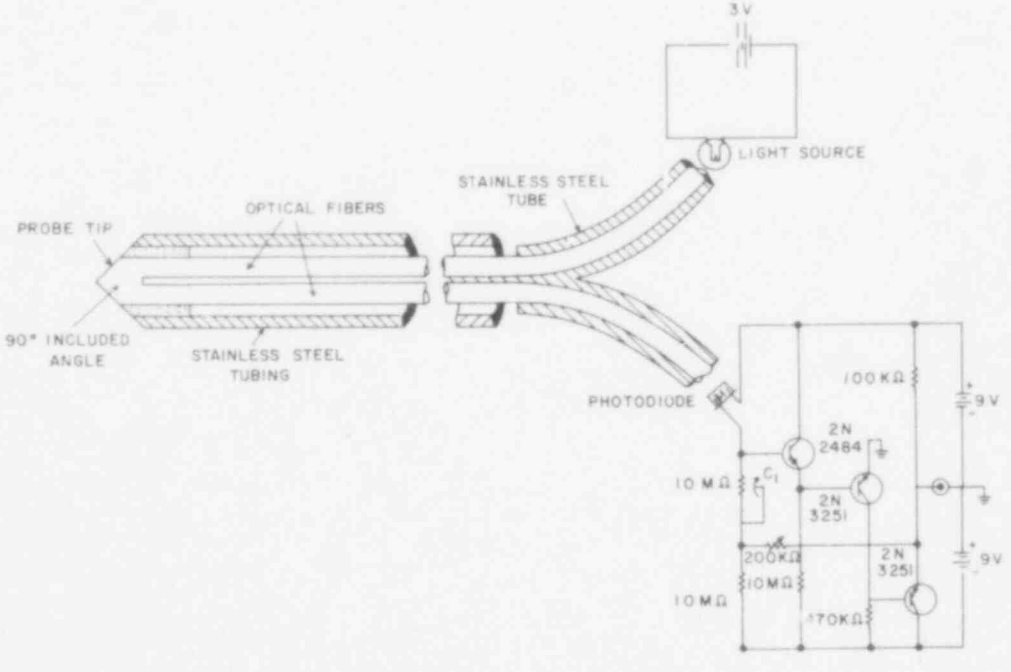

Figure 2. Schematic representation of the optical probe. (BNL Neg. No 1-641-78).

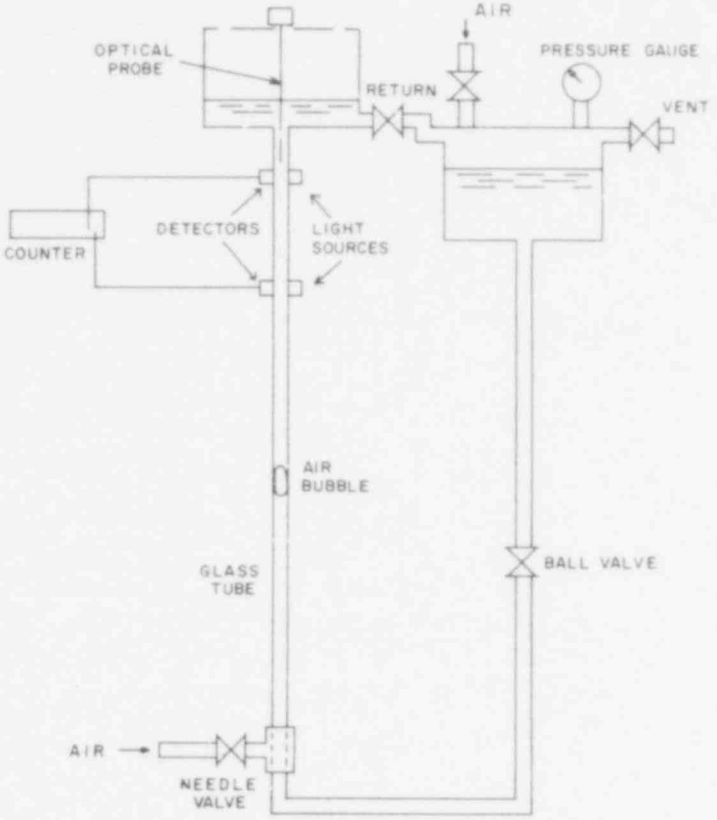

Fig. 3 - Experimental set-up for Probe Calibration at Low Velocities.
(BNL Neg. No 1-651-78)

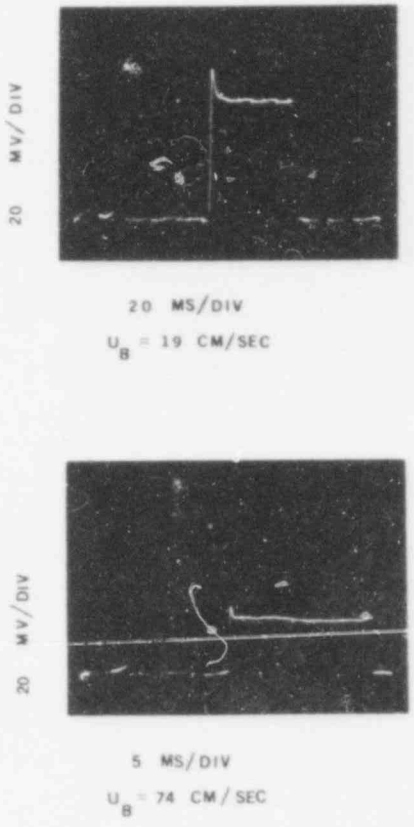

Fig. 4 - Typical Output of the Optical Probe.
(BNL Neg. No 9-111-77)

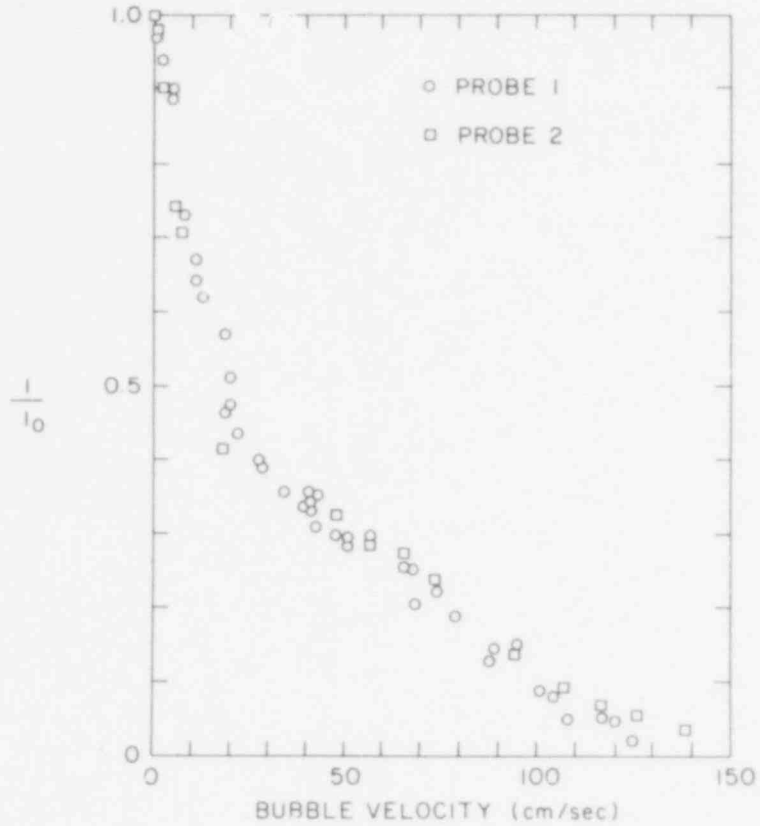

Fig. 5 - I/I_0, Probe Signal at a Given Bubble Velocity Divided by the Steady Signal in Air. (BNL Neg. No 1-650-78)

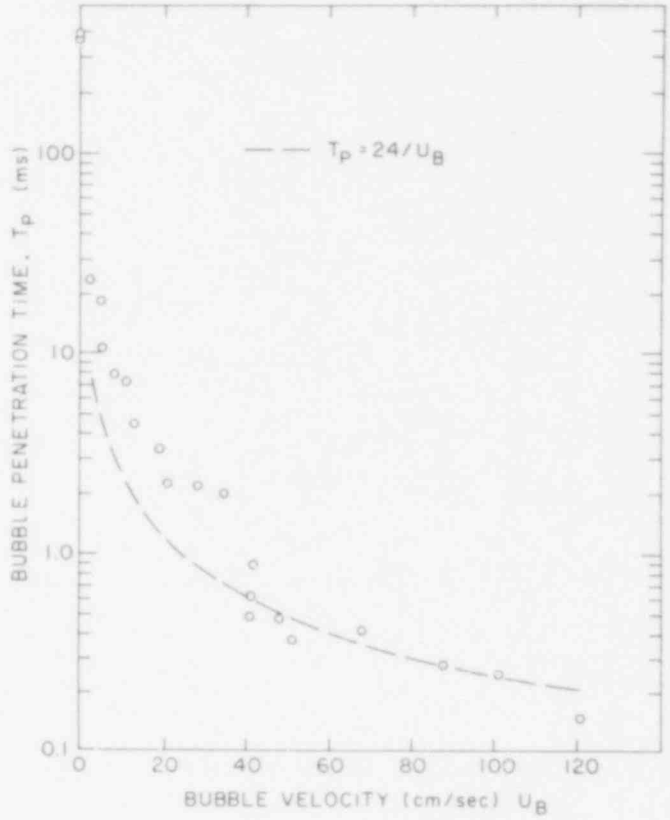

Fig. 6 - Bubble Penetration Time vs. Bubble Velocity. (BNL Neg. No 1-643-78)

In order to study the effect of tip geometry, an optical probe with a tip similar to the one used by Danel and Delhaye (1971) was built (Figure 7) and checked in the same calibration loop presented in Figure 3. Typical outputs are presented in Figure 8. An important observation to be mentioned is that the probe signal output does not go zero as in the previous case, when the probe tip is immersed in water. The net output, I, divided by the steady net output in air, I_o, is plotted in Figure 9 as a function of bubble velocity. The attenuation of the signal observed is less for this geometry than the one previously presented in Figure 5. The penetration times, Figure 10, for the U-shaped probe tip geometry show a similar variation to the ones observed previously, (Figure 6). At high velocities $U_B > 40$ cm/sec, they are 33 percent longer showing a strong effect of the tip geometry.

The flat face optical probe with 90^o total angle was also checked at the high velocity air-water loop shown in Figure 11 (Leonhardt, 1977), in the horizontal position. Figure 12 shows some typical results of the probe output for superficial water velocities of 6.8 m/sec. The reason for this behavior is due to the change in the relative direction of the gravity field with respect to the probe axis and with respect to the shear and surface tension forces acting.

In order to methodically study the geometrical optics and response characteristics of various probe geometries, a computer program was written. The program sets up a given probe tip geometry, half circle or linear (Figure 13). It then divides the incoming fiber ($n_{glass} = 1.62$) into N equal segments. From each point, x_o, y_o, rays of light traveling as straight lines and making an angle , with the vertical axis are drawn. The

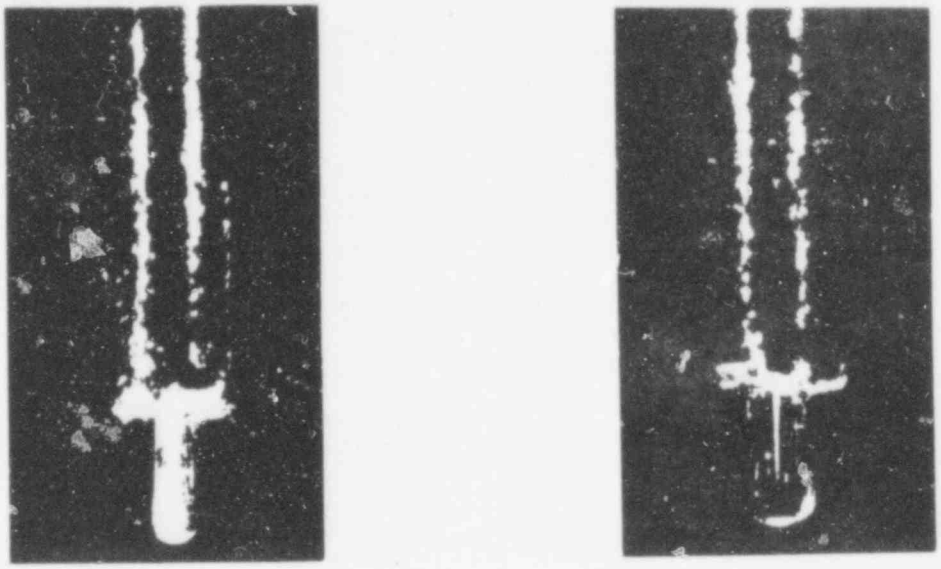

A B

OPTICAL FIBER DIAMETER 0.125 MM , ST. STEEL TUBE O.D. 0.500 MM.

Fig. 7 - Photographs of U-Bend Optical Probe Tip. (BNL Neg. No 1-653-78)

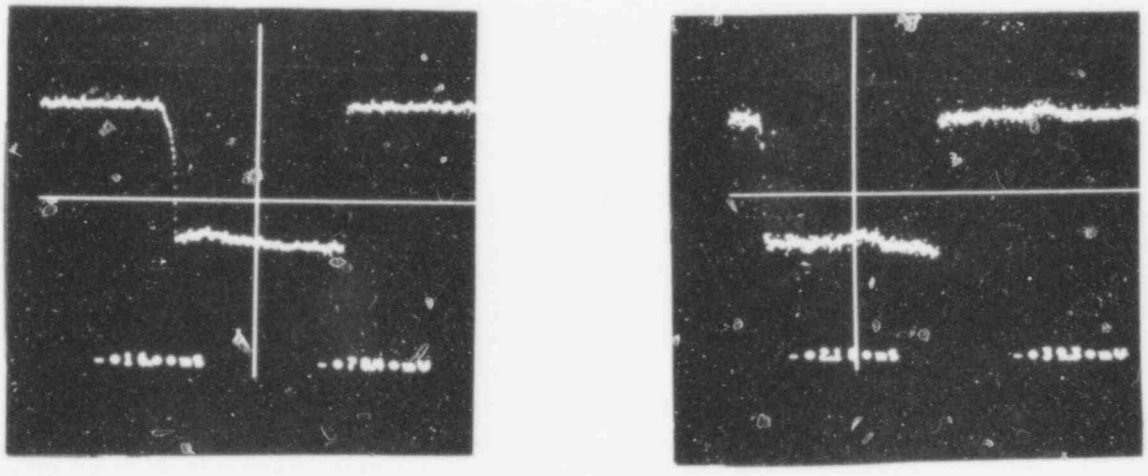

A.

Bubble Velocity = 10 cm/sec
Steady Signal in Water = -76 mV
Steady Signal in Air = -184 mV

B.

Bubble Velocity = 184 cm/sec
Steady Signal in Water = -80 mV
Steady Signal in Air = -155 mV

Fig. 8 - Typical Oscillograms of the U-Bend Optical Probe.
(BNL Neg. No 1-654-78)

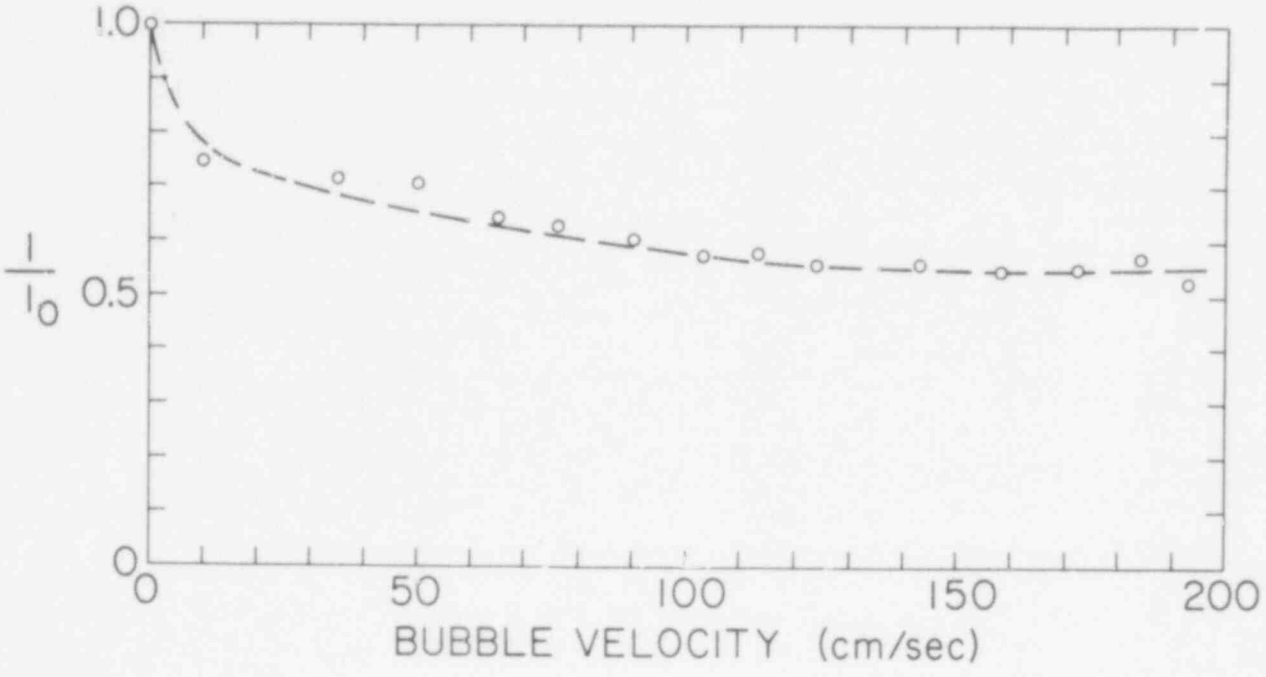

Fig. 9 - I/I_0, Ratio of Net Signal Output Divided by Net Output in Air vs. Bubble Velocity for U-Bend Probe. (BNL Neg. No 1-647-78)

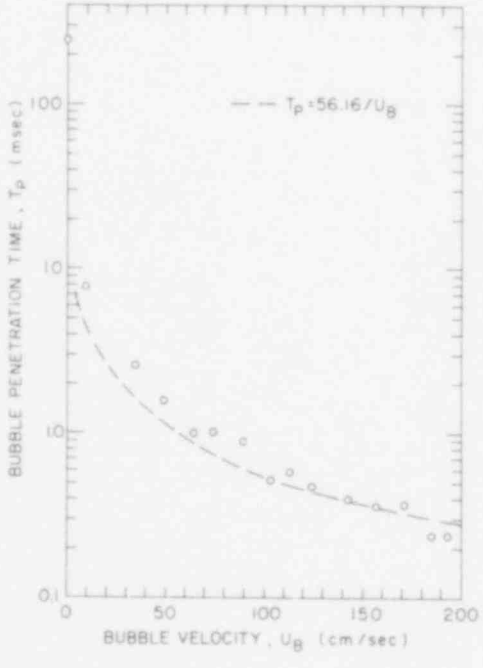

Fig. 10 - Penetration Time vs. Bubble Velocity for U-Bend Probe. (BNL Neg. No 1-648-78)

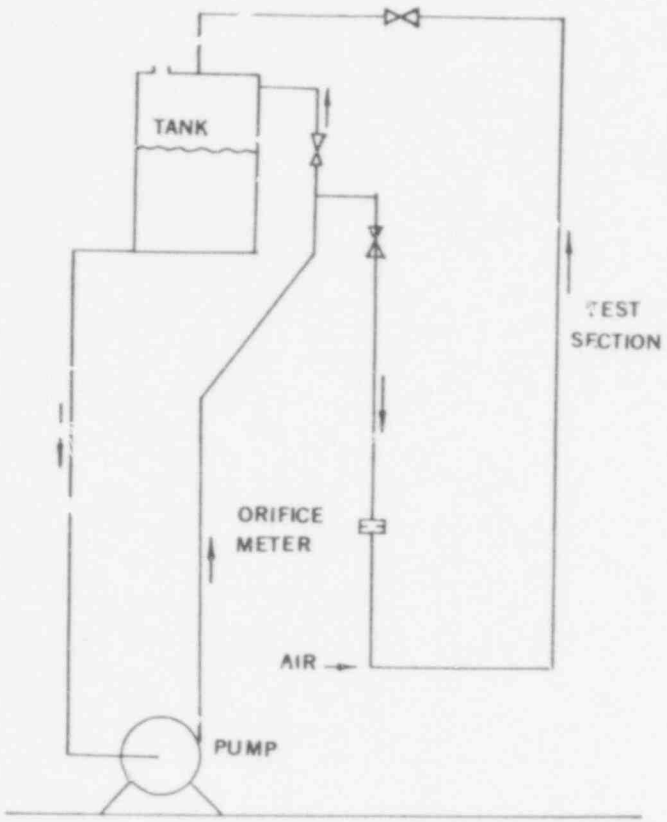

Fig. 11 - Schematic of High Velocity (U_B < 7 m/sec) Calibration Air Water Loop.
(BNL Neg. No 4-919-78)

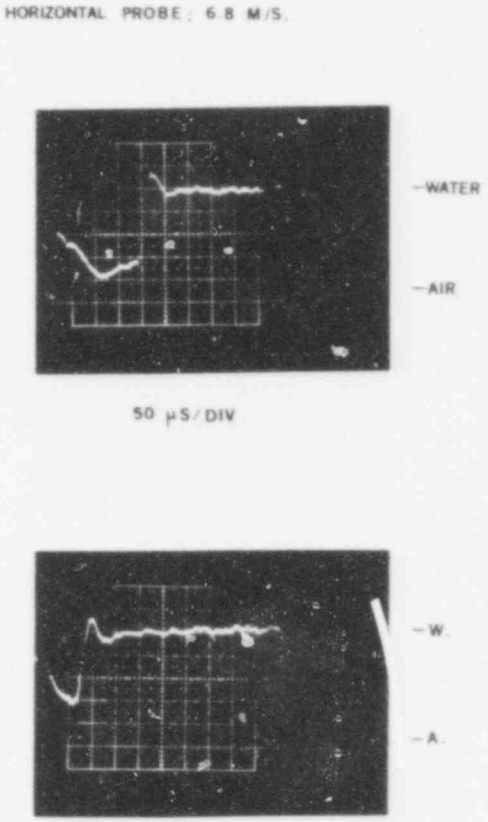

Fig. 12 - Typical Output of Straight Edge Optical Probe in Horizontal Position.
(BNL Neg. No 3-1765-78)

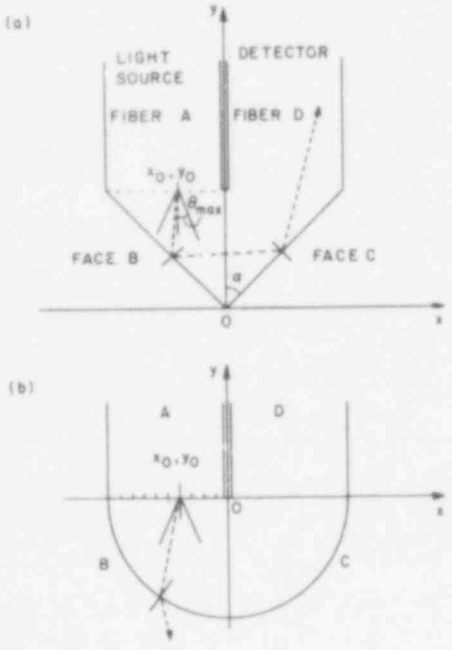

Fig. 13 - Schematic Representation of the Probe Tip for Computer Program. (BNL Neg. No 1-644-78)

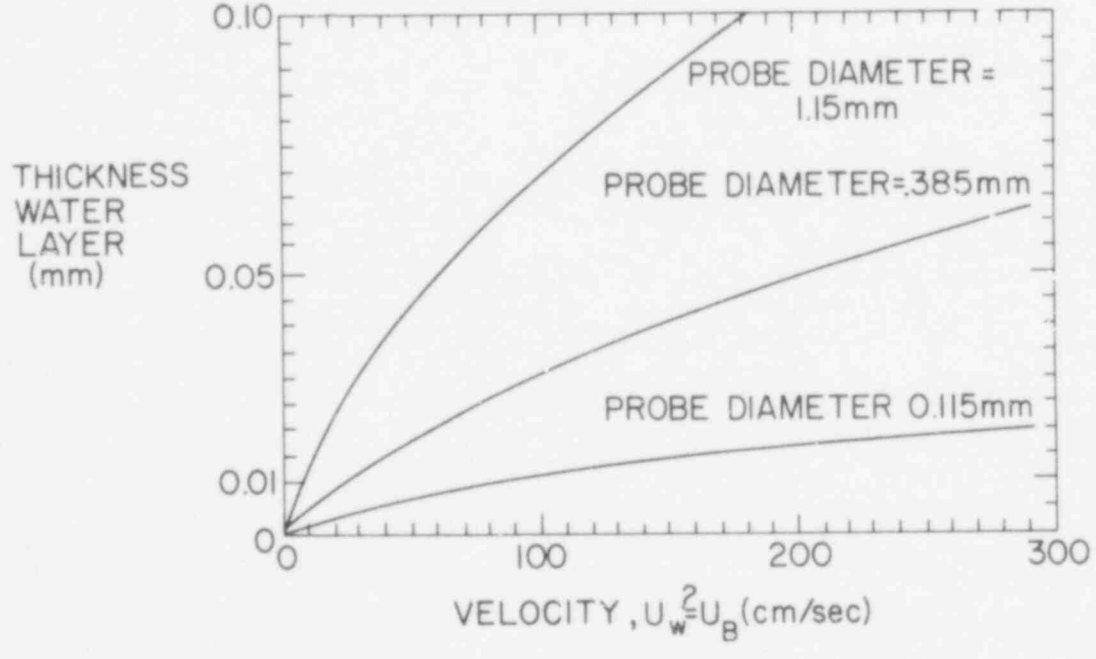

Fig. 14 - Plot of Water Layer Thickness vs. Wire Withdrawal Velocity for Three Probe Diameters. (BNL Neg. No 3-1723-78)

angle θ is varied from $-\theta_{max}$ to $+\theta_{max}$ in half degree increments. The value of θ_{max} is determined from the numerical aperture or acceptance cone provided by the optical fiber manufacturer. For our case, this was chosen as 30^{o}. The program determines the intersection point of the specific light ray and the face B. At that point, Snell's law is applied to decide whether the ray is refracted out or reflected back assuming the probe tip to be in water or in air. The ray, if reflected, is followed to face C. The same procedure is applied to decide the refraction or reflection at point C. If the ray is once again reflected, and is traveling towards the detector D, the geometry is once again checked for refraction along the fiber assuming that the fiber is in air. Some of the rays reflected from the face B can also return through the fiber A. Keeping a close account of the rays which were initiated and the rays lost at A, B, C, or D, one is able to calculate the percent of the rays which go to the detector and provide a useful output signal. The probe response was investigated in air and in water as a function of the probe tip angle, and the acceptance angle, (Abuaf, et al. 1978a). The calculations were also extended to study the signal attenuation that would be experienced when a variable film thickness is present at the probe tip (Abuaf, et al. 1978b).

A possible explanation for the probe output behavior for various bubble velocities was presented by Abuaf (1977c). A water film thickness left on the probe tip and increasing with the bubble velocity was thought to explain that the computer program can provide a measure of the signal decrease with water layer thickness, one can calculate and predict a probe behavior similar to the one experimentally observed by combining the two predictions. Figure 14 is a plot of the water layer thickness as a function of wire withdrawal

velocity as calculated from the theoretical predictions of White (1968) and Tallmadge (1967), for three cylindrical tube diameters. In Figure 15, the attenuation of the light signal reaching the detector normalized to its steady maximum value in air is presented as a function of the water layer thickness, δ (mm) for a 0.125 mm fiber. The results shown are obtained from a computer program and apply to two ranges of the acceptance angle $-30^{o} < \theta < 30^{o}$ and $-5 < \theta < 5^{o}$. Combining figures 14 and 15, we obtain a cross plot of the normalized signal, I/I_{o}, vs. the withdrawal velocity assumed to be equal to the bubble velocity (Figure 16). The decrease of I/I_{o} vs U_{ω} is very similar to the one observed experimentally and reported in Figures 5 and 9. This reasoning and results show that our physical understanding of the optical probe behavior is reasonable.

b. The r-f Probe. In parallel to the optical probe, a second probe operating on a radio-wave frequency (r-f probe) was also developed, built and is being tested (Abuaf, et al., 1977c). The probe (Figure 17) consists of two shielded insulated wires. One of the wires is used as an emitter and fed a sine wave. The second wire is used as a receiver or antenna, and the output is fed to an oscilloscope after proper amplification. The probe output depends upon whether or not the two wires at the tip are immersed in water or in air. A static calibration of the probe output in the low velocity calibration loop, Figure 3, showed that the output varies with the input frequency, Figure 18. The probe seems to act as a band-pass filter. The output also varies linearly with the immersion depth along the nonshielded parts of the wires. The probe with a 500 kHz, 23 v ptp sine wave input was tested in the set up shown in Figure 3. The bubble velocity and size were also recorded

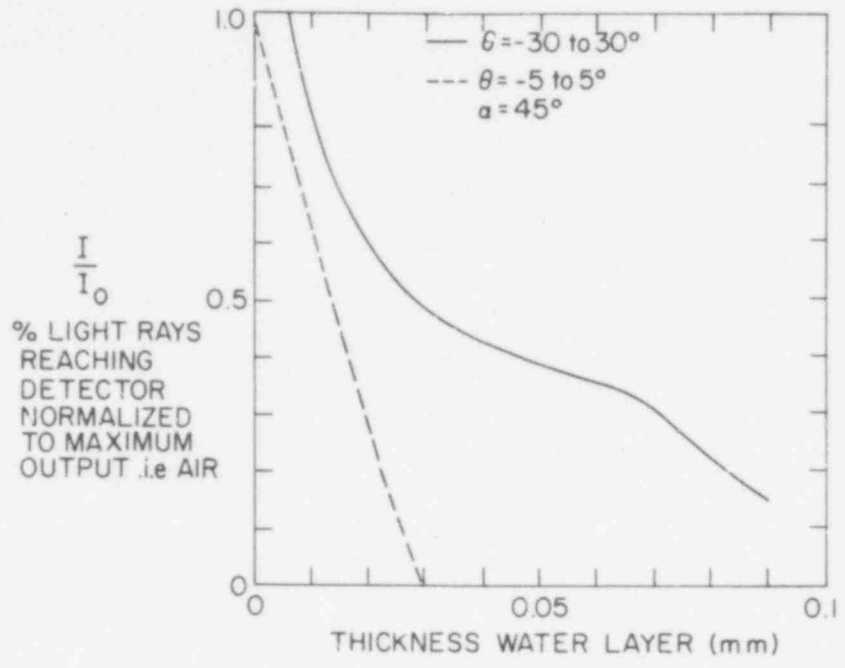

Fig. 15 - Normalized Probe Signal Attenuation as a Function of Water Layer Thickness. Calculated from Computer Output for a 0.125 mm Fiber. (BNL Neg. No 3-1721-78)

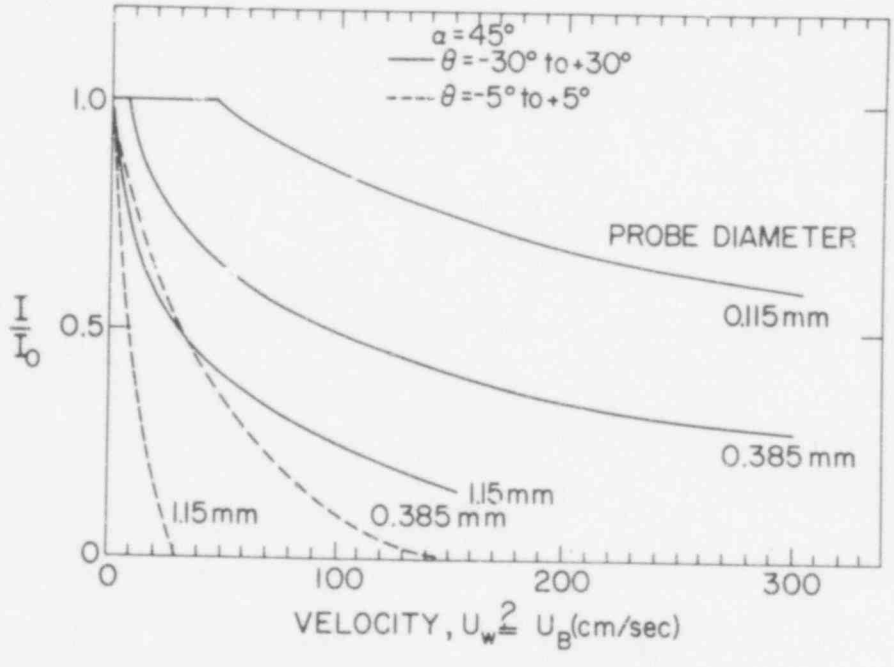

Fig. 16 - Cross Plot of the Normalized Probe Signal vs. Wire Withdrawal Velocity for Three Probe Diameters and Two Values of the Acceptance Angle. (BNL Neg. No 3-1719-78)

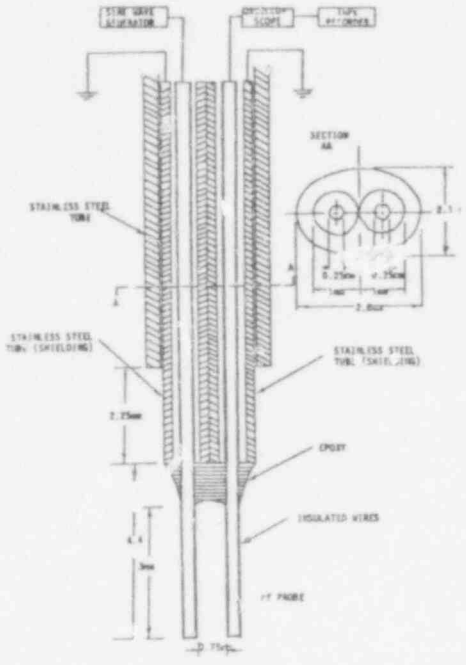

Fig. 17 - Schematic Representation of the r-f Probe. (BNL Neg. No 4-920-78)

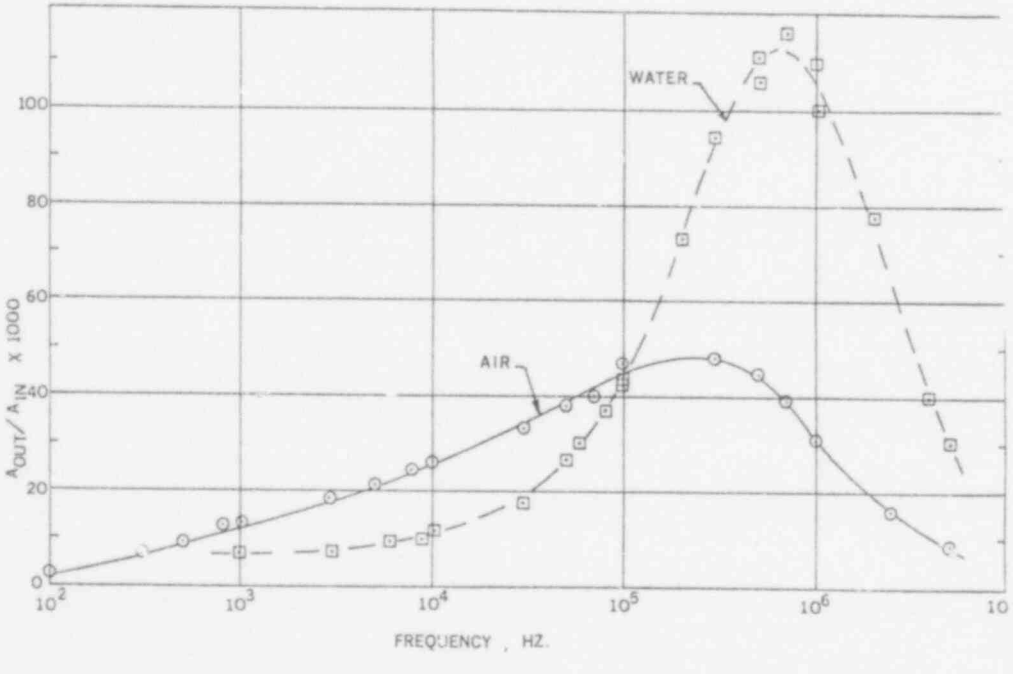

Fig. 18 - Ratio of r-f Probe Output to Input as a Function of Input Wave Frequency. Probe Tip in Air and in Water, Checked in Low Velocity Calibration Set Up. (BNL Neg. No 4-915-78)

independently by two light sources and detectors. Typical outputs are shown in Figures 19 and 20. Figure 21 is a zoom-graph of the r-f probe response during the passage of the bubble. The response of the probe appears to be consistent under the dynamic or static operation conditions. Figure 22 shows a comparison between the bubble velocities as determined by the r-f probe and the output of the two light sources-two detectors set-up. The agreement is satisfactory.

Considering the void fraction measurements, Figure 23 depicts agreement between the bubble sizes as determined by two independent methods (r-f probe and two light sources detectors) as a function of bubble velocity. The r-f probe seems to have a relatively simple construction and once tuned properly to the experimental geometry, seems to provide the necessary information (void fraction and interface velocity).

GLOBAL INSTRUMENTS

The global instruments for measuring the chord averaged void fraction consists of five channels of γ sources (Thulium 170, half life of 127 days, and 0.084 Mev) and Cadmium Telluride detectors. Sources having a strength of 30 ci should yield a one standard deviation of $\sim$ 1.5 percent in a 1.0 ms sample at the detector. The five channels are provided with the proper collimation to have a measuring area of 2 x 2 mm^2 and will have the ability to traverse the test section both in axial and transverse directions.

DATA ACQUISITION AND DATA ANALYSIS SYSTEMS

The centralized Data Acquisition and Data Analysis System (DADAS) was designed as a real time digital data system with multiterminal multitasking

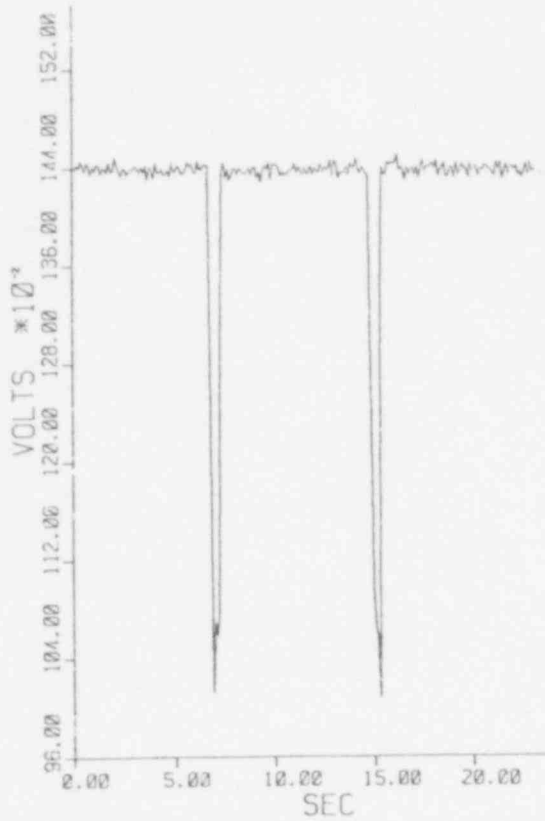

Fig. 19 - Typical Output of Two Light Sources-Detectors During Passage of a Bubble.
(True Time = Time x 7.5/120)
(BNL Neg. No 4-912-78)

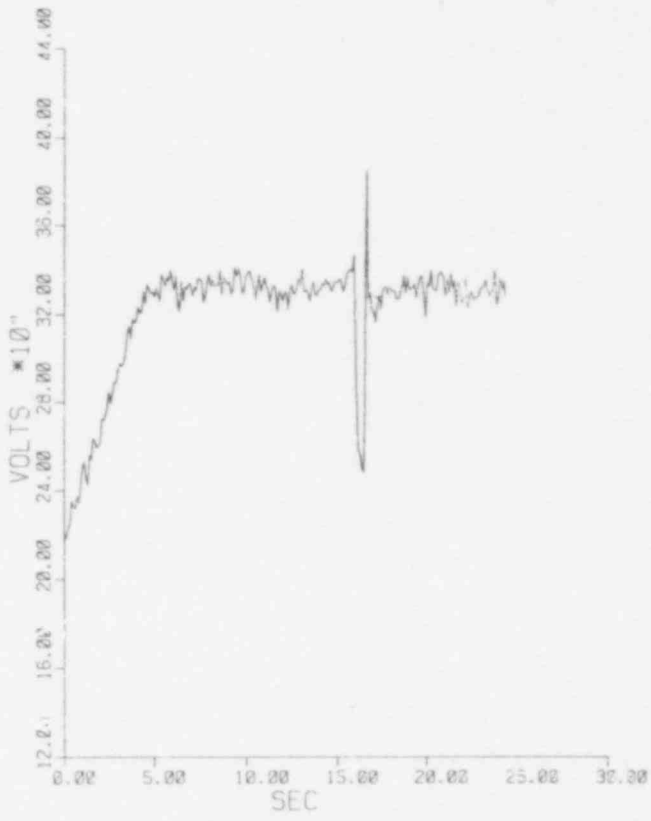

Fig. 20 - Typical [illegible]-f Probe Output.
True Time = Time x 7.5/120
(BNL Neg. No 4-913-78)

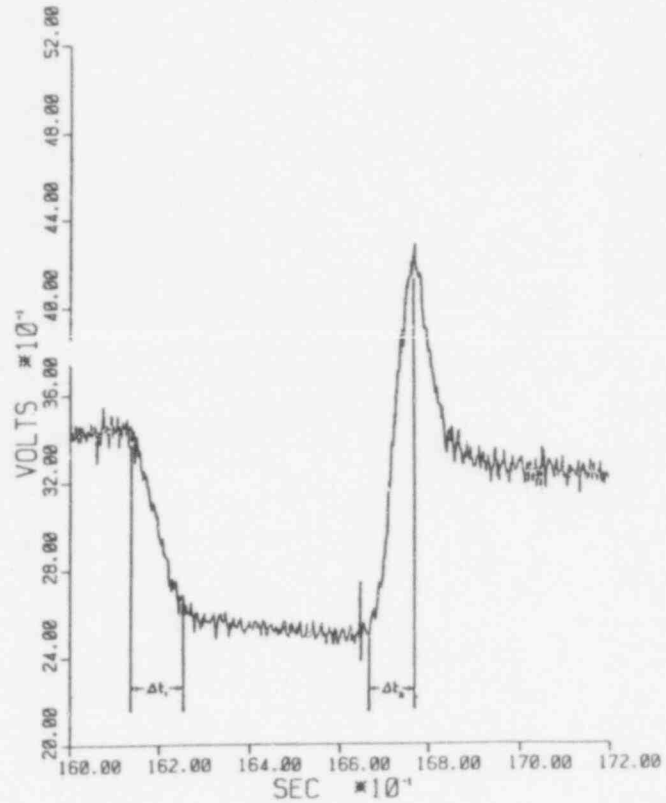

Fig. 21 - Typical Expanded r-f Probe Output.
(BNL Neg. No 4-914-78)

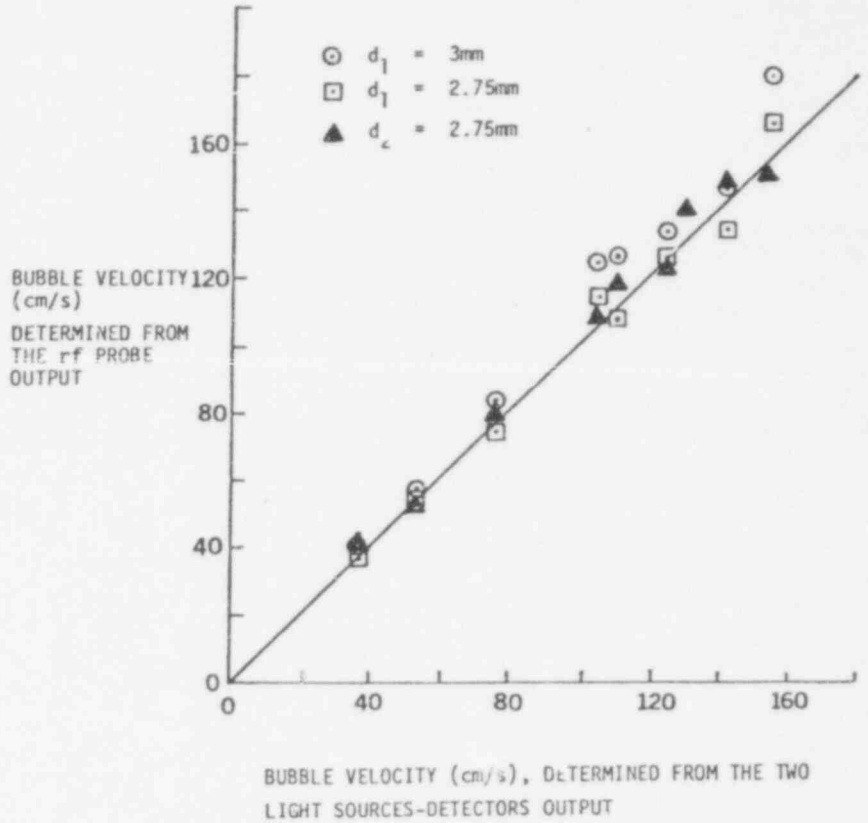

Fig. 22 - Comparison of Bubble Velocity as Determined by Two Independent Methods (r-f Probe and Two Light Sources Detector)
(BNL Neg. No 4-917-78)

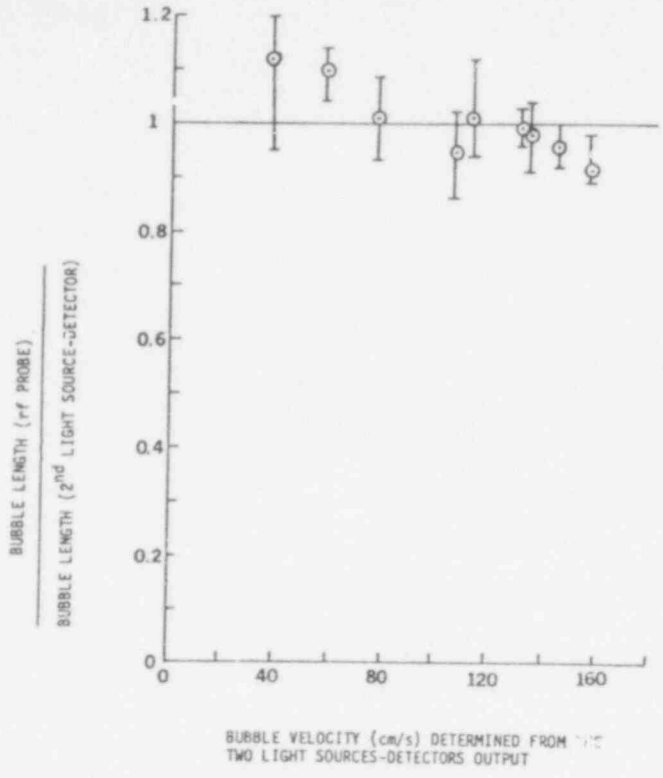

Fig. 23 - Ratio of Bubble Length as Determined by the r-f Probe and the Two Light-Sources-Detectors as a Function of Bubble Velocity. (BNL Neg. No 4-918-78)

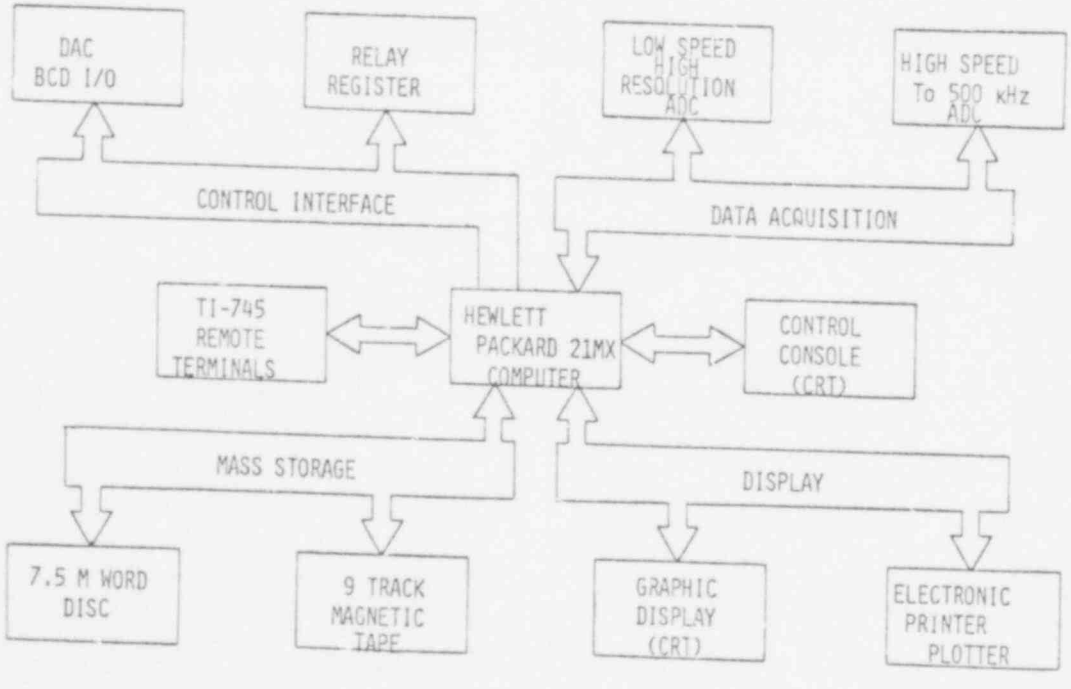

Fig. 24 - Schematic Representation of Data Acquisition System. (BNL Neg. No 4-916-78)

capability. The system was constructed around a Hewlett Parckard 9640 system 1000 consisting of a 21MX minicomputer with 112 kilowords of central memory, 7.5 megaword cartridge disc, 9 track magnetic tape transport and paper tape I/O. Central control of the system is accomplished with a CRT terminal while the 3 satelite stations employ silent 700 terminals. Tabular and graphical presentation of data is achieved with a Varian electrostatic printer/plotter capable of listing 600 LPM and plotting 1.6 ips. Interface of the ADC systems is both direct, an interface per device, and via the universal interface bus, IEEE standard 488 (Figure 24).

Three levels of ADC speed and resolution are incorporated within DADAS. The slow speed, high resolution system employs an integrating digital voltmeter with microvolt resolution and 300 channel guarded crossbar scanner. The through-put rate of this system is up to 18 measurements per second with high common mode voltage rejection capability. The intermediate speed system is a 15 bit ($\pm$ 10.24 volts) multiplexed ADC with a 50 KHz through-put rate. The system employs a single programmable gain amplifier and a signal conditioning amplifier and filter per channel. The system has high common mode voltage rejection capability and can be connected directly to experiments. The high speed system is also a 15 bit ($\pm$ 10.24 volt) multiplexed ADC with a 500 KHz through-put rate. The system has 8 input channels with simultaneous sample and hold amplifiers. This sytems was designed specifically for digitizing analog tapes.

A software system is currently under development which utilizes the ADC systems to generate a 1.25 megaword data base. The data base can then be broken up into blocks which represent a smaller time frame within total time of data base. The block size is variable from 128 data words to 2048 data words and the time step between data words within the block can be any factor of 20

microseconds. The system permits mathematical manipulation of both the data block and the contents of the data block. The results of the block analysis can be displayed in both tabular and graphical form as required. In the signal analysis work, time and frequency domain data manipulation software was integrated into the block system with the needed real and complex mathematics. Concerning the methods for correlation incoherencies in data acquisition hardware, an analytical method was presented based on the cross correlation function. A computer program was written, incorporated into the system, and an example was solved where time incoherency between two recording channels was determined (Abuaf, et al 1977c). A program that computes the discrete Fast Fourier Transform of a time series was also added to the package. The same program also allows calculation of the inverse Fourier Transform. Using these subprograms, a typical signal enhancement procedure was set, and an example was solved. This last program allows the reconstruction of input functions to instruments once the output and the instrument transfer functions are known (Abuaf, et al 1977c).

SUMMARY

In summary, one can state that with respect to local probes:

- An optical probe was developed, constructed and its response to bubbles was investigated.
- A computer program was written to study the probe response characteristics and determine the optimum probe geometry.
- The new design being encased in stainless steel is less fragile and can withstand more difficult conditions.

402 289

- It was shown that with proper calibration a single probe could give both interface velocity and void fraction in the velocity range studied.
- A potential physical explanation for the optical probe behavior has been identified.
- An r-f probe was also developed, constructed and its calibration was executed.

A block signal analysis system was developed and time and frequency domain data manipulation software was integrated and applied to some specific problems.

REFERENCES

1. Danel, F. and Delhaye, J. M., "Sonde Optique pur Mesure du Taux de presence Local en Ecoulement Diphasique," Measures-Regulation-Automatisme Auot-Septembre 1971.

2. Hinata, S., "A Study of the Local Void Fraction by the Optical Fiber Glass Probe," Bull JSME, 15, 1972.

3. Jones, O. C., Jr., "BNL Light Reactor Thermohydraulic Development Program: Instrumentation Tasks," 1977, BNL-NUREG-22588.

4. Abuaf, N. and Swoboda, A., "Reactor Safety Experimental Program: Quarterly Progress Report for the period January-March 1977," BNL-NUREG-50661, p. 149, 1977a.

5. Abuaf, N. and Swoboda, A., "Reactor Safety Experimental Program: Quarterly Progress Report for the period April-June 1977," BNL-NUREG-50683, p. 160 1977b.

6. Abuaf, N., et al., "Reactor Safety Experimental Program: Quarterly Progress Report for July-September 1977," BNL-NUREG-50747, 1977c.

7. Miller, N. and Mitchie, R. E., "The Development of a Universal Probe for Measurement of Local Voidage in Liquid Gas Two-Phase Flow Systems," Eleventh National ASME/AIChE Heat Transfer Conference, Minneapolis, 1969.

8. Tallmadge, J. A. and White, D. A., "A Gravity Corrected Theory for Cylinder Withdrawal," AIChE J., 13, 4, 1967.

9. Leonhardt, W. J., et al., "Reactor Safety Experimental Program: Quarterly Progress Report for the period July-September," BNL-NUREG-50747, 1977.

10. Abuaf, et al., "Reactor Safety Experimental Program: Quarterly Progress Report for the period October-December 1977," BNL-NUREG- , 1978a.

11. Abuaf, N. and Sweeney, L., "Reactor Safety Experimental Program: Quarterly Progress Report for the period January-March 1978," BNL-NUREG- , 1978b.

12. White, D. A. and Tallmadge, J. A., "Film Properties and Design Procedures in Cylinder Withdrawal," I & EC Process Design and Development, 7, 4, 503-508, 1968.

402 291

DISTRIBUTION LIST

G. Bagchi, NRC
D. Basdekas, NRC
V. Benaroya, NRC
C. Burger, NRC
R. T. Curtis, NRC
S. Fabic, NRC
D. Fischer, NRC
Y. Y. Hsu, NRC
W. Y. Kato, BNL
C. N. Kelber, NRC
H. J. Kouts, BNL
R. Mattson, NRC
A. W. Serkiz, NRC
L. Shao, NRC
M. Silberberg, NRC
L. Thompson, NRC
H. Todosow, BNL
L. S. Tong, NRC
R. W. Wright, NRC
N. Zuber, NRC

BNL RSP Division Heads
BNL RSP Group Leaders
BNL RSE Modeling Group

U.S. NRC Division of
Technical Information
and Control